Design and Analysis of a CMOS Based MEMS Accelerometer

Matthew A. Zeleznik
Microelectronic Engineering
Rochester Institute of Technology
Rochester, NY 14623

Abstract– Traditionally, microelectromechanical systems (MEMS) have been fabricated using standard surface micromachining or bulk micromachining processes with prior or subsequent CMOS incorporation. Recently, a new hybrid technique known as CMOS micromachining has been developed allowing for parallel fabrication of mechanical and electrical components. A single axis and dual axis accelerometer have been designed for submission for an ASIMPS alpha run using the CMOS micromachining process. Electrical and mechanical analysis and simulations for the single axis accelerometer have been performed. The sensitivity of the single axis accelerometer has been calculated to be 19.66mV/g neglecting the effects of parasitic capacitance. The released die has been packaged at RIT and a testing method has been determined and modeled.

1. INTRODUCTION

With the development of microelectromechanical systems, the ability to sense and actuate at the microscale level has been realized. Incorporation of electronic circuitry has allowed for mechanical signals to be converted to equivalent electrical signals providing information and an interface between electrical processing units and the outside world. Conversely, electrical signals can also be generated and converted into mechanical signals through the micromechanical components to thus act upon and influence the outside world. Because of the similar scale between integrated circuits and micromachined devices, IC processing technology has been adapted for the fabrication of the latter.

In general, two types of process have been used to manufacture microelectromechanical systems. The first type of process, known as surface micromachining, utilizes various thin films and a sacrificial layer, deposited and patterned on a silicon wafer to create the structural layers of the device. The sacrificial layer is then etched away; releasing the upper layers and creating a freestanding device. In contrast, bulk micromachining utilizes the thickness of a silicon wafer to create the micromachined structures. In a bulk micromachining process, a masking layer is deposited and patterned on the silicon surface and the substrate is then selectively removed to create the micromachined structures. While each of these techniques lends itself to the fabrication of micromechanical components, the incorporation of the signal and control circuitry has had to be done off chip or with a prior or subsequent CMOS process.

Recently, a hybrid technique for fabricating MEMS devices, known as CMOS micromachining, [1] has been developed. With the CMOS micromachining process wafers are fabricated using any standard CMOS process. By devoting a section of the chip, void of electronics, the micromechanical structures are defined using the metal and dielectric layers for the CMOS interconnects. An anisotropic etch is then performed through the unmasked regions of the dielectric layers. Trenches are subsequently etched into the exposed substrate using a deep reactive ion etch (DRIE). An isotropic SF_6 plasma etch is then used to remove the silicon underneath the metal and oxide interconnects thus releasing the mechanical components. The process flow is illustrated in figure 1.

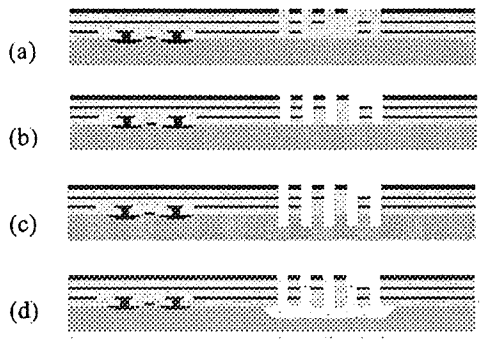

Figure 1: Illustration of the CMOS based MEMS process. (a) CMOS processed wafer. (b) Anisotropic oxide etch through the dielectric layers. (c) DRIE into silicon substrate. (d) SF_6 release of metal/oxide structures.

In an effort to promote the fabrication of prototype MEMS devices, the Department of Advanced Research Projects Agency (DARPA) is partially funding foundry runs for the new CMOS process, allowing end users to design their own chips for fabrication. Using Cadence and specific design rules developed by Carnegie Mellon University [2] a single axis and dual axis accelerometer based on an adaptation of the ADXL series accelerometer by Analog Devices, Inc. were designed for the Fall 2000 Application Specific Integrated MEMS Processing Service (ASIMPS) alpha run.

2. DEVICE DESIGN

The ADI style accelerometer consists of three basic components as illustrated in figure 2. By using Newton's second law, which states that the force is equal to the product of the mass of an object and an applied acceleration, it is possible to detect an external acceleration through a measured force. In order to measure the force, two sets of interdigitated comb fingers, rotor and stator, are suspended from a proof mass supported by the mechanical springs and outer frame. The springs are designed to provide mechanical support for the suspended structure and to allow for the deflection of the proof mass in response to an applied acceleration. In turn, proof mass is designed such that a significant mass is present for response to an acceleration as well as providing an anchor point for the rotor fingers which form the electrodes of the parallel plate capacitors. Under an applied acceleration, the proof mass will deflect causing a change in capacitance between the stator fingers and the rotor fingers. Since capacitance is a measure of the electrical force, the mechanical energy in the system can be converted into an electrical signal representative of the magnitude of the acceleration.

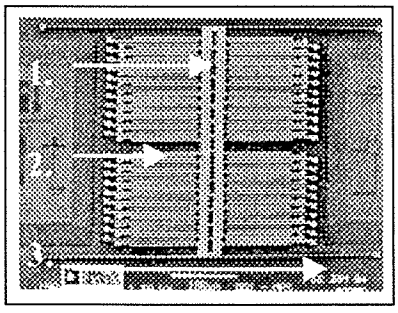

Figure 2: SEM of ADI accelerometer showing the proof mass (1), electrodes (2) and springs (3). [3]

The mechanical sensitivity of the device can be tailored, through the spring constant, by controlling the amount of deflection for a given mass and acceleration. In order to provide the maximum sensitivity for the device the distance between the stator fingers and the rotor fingers should be minimized and the cross sectional area should be maximized. To ensure that the electrodes do not become electrically shorted under a large acceleration, the gap must be larger than the maximum deflection of the springs. Alternatively, grounded limit stops must be incorporated into the design such that the gap between the limit stops is slightly less than the electrode gap.

As part of the adaptation of the ADI accelerometer [4] which this design was based upon, an outer frame is utilized for the anchor point of the stator fingers in order to match the out of plane curl induced by thermal stresses in the bimorph structures of the released layers. Additionally, certain structures were designed in order to adhere to the MEMS design rules for the die submission. Ideally, the parasitic capacitances, consisting of the substrate to device capacitance, interconnect capacitance and bondpad capacitance, should be minimized.

By routing the electrical interconnects through the mechanical structures using the first and second metal layers, a full capacitive bridge can be realized. Two input signals, 5V pulsed waves at a frequency of 1MHz, are applied 180 degrees out of phase. The signals are applied to every other movable electrode by routing the electrical signal through the springs and proof mass. The output signals, positive and negative, are extracted from the fixed electrodes. Figure 3 shows a detail of the electrode layout as well as the equivalent circuit model.

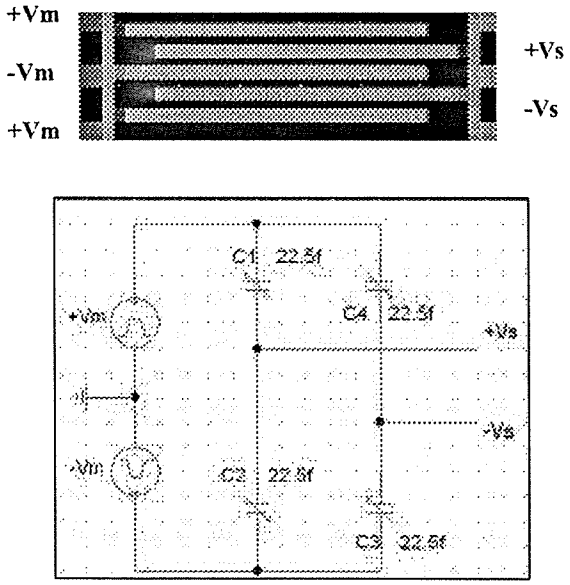

Figure 3: (a) Electrode layout and signal designation. (b) Equivalent circuit model.

3. MODELING

A. Mechanical Modeling

A simplified mechanical model for the spring system can be obtained by treating each beam as a simple cantilever and using force methods to extract the spring constant. In this analysis it is assumed that the effects of the trusses in each spring are negligible. Using Hooke's Law for a single cantilever, the spring constant can be defined as

$$k = F/\delta \qquad (1).$$

Substituting the displacement as function of force gives the spring constant for a single beam in the spring system as

$$k = \frac{3EI}{l^3} \qquad (2),$$

where E is Young's Modulus of the material and I is the moment of the beam in the z direction, given by

$$I = \frac{wh^3}{12} \qquad (3).$$

Since each spring consists of four beams, the spring constant becomes one quarter of the individual spring constant. The entire spring system consisting of four sets of springs is then four times the spring constant of each spring set which can be expressed as follows

$$k = \frac{E(wh^3)}{4l^3} \qquad (4).$$

A more advanced model, which takes into account the effects of the trusses on the spring constant, was derived by Fedder [5] using energy methods. By applying Castigliano's second theorem to the individual components of each spring an equation for the overall spring constant of the system was found to be

$$k = \frac{48EI_b[(\tilde{a}+l_b)n-l_b]}{l_b^2(n-1)[(3\tilde{a}^2+4\tilde{a}l_b+l_b^2)n-l_b^2]} \qquad (5),$$

where n is the number of trusses in each spring, l_b is the length of the beam and $\tilde{a}$ is given by the ratio of the beam moments

$$\tilde{a} = \frac{I_b l_t}{I_t} \qquad (6).$$

By taking the limit of equation 5 as $\tilde{a}$ goes to zero, it can be shown that equation 5 is four times larger than equation 4. Closer analysis suggests that the constant factor in equation 5 should be changed to 12 giving the spring constant for the system

$$k = \frac{12EI_b[(\tilde{a}+l_b)n-l_b]}{l_b^2(n-1)[(3\tilde{a}^2+4\tilde{a}l_b+l_b^2)n-l_b^2]} \qquad (7).$$

B. Electrical Modeling

Since each capacitor in the full bridge will change as a function of the gap distance, the capacitance can be written as [6]

$$\Delta C = \frac{\varepsilon A}{g_o \pm y} = \frac{\varepsilon A}{g_o(1 \pm \frac{y}{g_o})} = \frac{\varepsilon A}{g_o}(1 \pm \frac{y}{g_o}) \qquad (8).$$

By applying Kirchoff's Current Law in the frequency domain at the positive output of the half bridge circuit, an expression for the output voltage can be expressed by

$$Vs = \frac{sC_1 - sC_2}{sC_1 + sC_2 + sC_p + \frac{1}{R_l}} Vm \qquad (9).$$

The sensitivity of the device can then be found by substituting C1 and C2 with the proper sign from equation 8 and realizing that the displacement, y, can be expressed as the ratio of the force to the spring constant giving

$$\frac{Vs}{a} = \frac{2Co}{2Co + Cp + \frac{1}{R_l}} \frac{m}{kg_o} Vm \qquad (10).$$

4. ANALYSIS AND SIMULATIONS

For the single axis accelerometer, the spring geometry which ultimately affects the spring constant can be found in table 1.

Table 1: Spring geometry

	Height	Width	Length
Beam	2.25um	2um	120um
Truss	2.25um	2um	4um

Using this geometry and a Young's Modulus of 61GPa [2] the spring constants were calculated using the force method (equation 4), the energy method (equation 5) and

the corrected energy method (equation 6). The results for the analysis of the spring constant are summarized in table 2.

Table 2: Spring Constant results

Method	K (N/m)
Force	0.159
Energy	0.505
Energy (Corrected)	0.122

IDEAS finite element analysis was performed in order to verify that the above spring constants were accurate. A solid model was constructed and a boundary condition was applied to the fixed end of the spring so that all motion was constrained. At the free end of the beam, a 1uN load was applied in the x direction. A plot of the displacement, shown in figure 4, was obtained. By noting the total displacement (28.2um) at the end of the spring, the spring constant was determined from equation 1. The resulting spring constant for the four spring set of 0.141N/m agreed well with the force model and corrected energy model. Because of the relative agreement between the three spring constants, the midpoint value of 0.141N/m was chosen for later calculations.

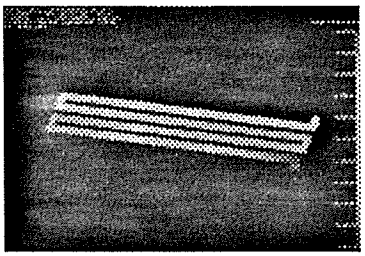

Figure 4: IDEAS FEA simulation results

For the 45um by 1.37um electrodes separated by a distance of 1.5um, the initial capacitance was calculated to be 19.25fF. The effective mass was calculated from the sum of the oxide mass of the rotor fingers and plate mass and the metal mass of the rotor fingers and plate mass. From equation 10, the sensitivity of the half bridge circuit with a 1GΩ load resistor was found to be 9.83mV/g neglecting the parasitic capacitance. For the entire bridge circuit the sensitivity was found to be 19.66mV/g.

Using PSpice, the full bridge circuit was simulated with a 1GΩ load resistor on the output from the positive and negative signal. A capacitive change of 0.37fF, corresponding to a 1g acceleration was simulated. The peak output of 186mV showed good correlation between the theoretical sensitivity and the output at 1g. Figure 5 shows the resulting waveform from the PSpice simulation. It should be noted that the decreasing output for each cycle is most likely due to the capacitors charging. Ideally, the output from each node should be fed into a switched capacitor op-amp so that charging effects are minimized.

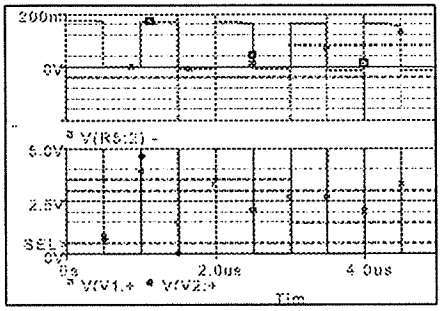

Figure 5: PSpice results for 1g acceleration.

5. TESTING METHODOLOGY

In order to test the device, the chip (figure 6) was packaged in a dual in-line package. Although no electrical tests were performed due to time limitations, a testing method has been developed. By placing the packaged chip at the end of a stainless steel cantilever beam, a time varying acceleration can be applied by deflecting the beam and allowing it to freely vibrate.

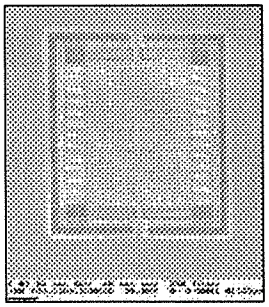

Figure 6: SEM of fabricated single axis accelerometer.

Simple vibration theory, which neglects the effects of damping, can be used to derive a theoretical equation for the acceleration. For a given beam, the deflection as a function of time can be expressed by

$$x(t) = x_o \cos(\omega_n t) \qquad (11),$$

where x_o is the initial displacement and ω_n is the natural frequency of the beam. Taking the first derivative of the displacement with respect to time yields an equation for the velocity as a function of time give by

$$\dot{x}(t) = \omega_n x_o \cos(\omega_n t) \qquad (12).$$

Taking the second derivative of the displacement with respect to time gives the time varying acceleration expressed as

$$\ddot{x}(t) = -\omega_n^2 x_o \cos(\omega_n t) \qquad (13).$$

For a stainless steel beam 25cm x 3cm x 0.5cm, the peak acceleration corresponds to approximately 0.5g. The time varying acceleration is plotted in figure 7.

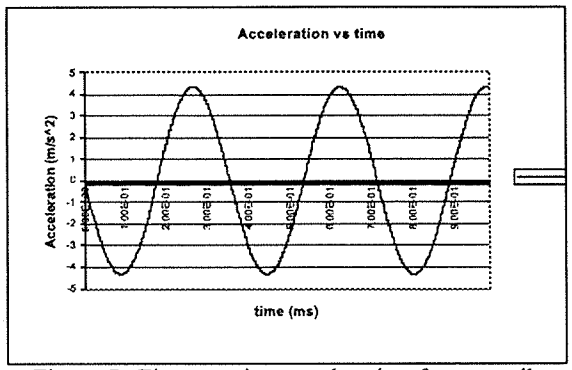

Figure 7: Time varying acceleration for a cantilever test structure.

For the actual device, it would be expected that the detectable acceleration would be significantly smaller than the theoretical results suggest. Since parasitic capacitances and the effects of curl were neglected in the analysis, the sensitivity of the device would be much lower than the calculated values. Additionally, the use of a resistive load will quickly cause a DC bias to form resulting in a damped output. A switched capacitor op-amp, donated by Mike Lu, was fabricated on chip and the outputs of one of the single axis devices were fed into the circuit. Although analysis was not performed on this circuit it would be expected that many of the problems associated with a resistive load would be alleviated yielding a working device.

6. CONCLUSIONS

A single axis and dual axis accelerometer were designed using the CMOS micromachining process. Careful modeling of the electrical and mechanical components demonstrated the ease of integration of two such systems at the theoretical level. Analytical evaluation of the single axis device showed good correlation with simulated results. A testing method, along with theoretical models has been presented and discussed. Future work includes analysis of the dual axis device in an analogous fashion, optimization of the test apparatus and testing of the device.

REFERENCES

[1] G.K. Fedder, S. Santhanam, M.L. Reed, S.C. Eagle, D.F. Guillou, M.S.-C. Lu, and L. R. Carley, "Laminated High-Aspect-Ratio Microstructures in a Conventional CMOS Process", *Proceedings of the IEEE Micro Electro Mechanical Systems Workshop*, San Diego, CA, Feb. 11-15 1996, pp. 13-18.

[2] G.K. Fedder, K.J. Gabriel and T. Mukerjee, "CMOS-MEMS Design for the Application Specific MEMS Process Service (ASIMPS)", presented at Carnegie Mellon University, Pittsburgh, PA, July 2000.

[3] http://www.coyotesystems.com/products/products.9.html

[4] H. Luo, G.K. Fedder and L. Richard Carley, "A 1 mG Lateral CMOS-MEMS Accelerometer", in *The 13th Annual International Micro Electro Mechanical Systems Conference* Miyazaki, Japan, Jan 23-27, 2000, pp. 502-507.

[5] G.K. Fedder, "Simulation of Microelectromechanical Systems", Ph.D. disseration, EECS, U. C. Berkeley, 1994.

[6] Y. Zhou, "Layout Synthesis of Accelerometers", M.S. thesis. Carnegie Mellon University, Pittsburgh, PA, 1998.

ACKNOWLEDGMENTS

The author would like to acknowledge Dr. Lynn Fuller for acting as project advisor, Andrew Randle for his help with FEA simulations, Dr. Tamal Mukherjee, Dr. Kaigham Gabriel, George Lopez, Hasnain Lackdawala and Mike Lu from Carnegie Mellon University and Dr. Kyle Lebouitz and Dr. Michele Migliuolo from XACTIX, INC. for funding, in part, of this work.

Matthew A. Zeleznik, originally from Pittsburgh, PA, received his B.S in Microelectronic Engineering from Rochester Institute of Technology in 2000. He has attained co-op work experience with Advanced Vision Technologies, Rochester, NY, the Center for Orthopedic Research at the University of Pittsburgh Medical Center and XACTIX, INC, Pittsburgh, PA. He will be attending graduate school at Carnegie Mellon as part of the MEMS group in the Department of Electrical and Computer Engineering in the fall of 2001.